View metadata, citation and similar papers at core.ac.uk

brought to you by CORE

provided by National Tsing Hua University Institutional Repository

The memory characteristics of submicron feature-size PZT capacitors with PtO_x top electrode by using dry-etching

This article has been downloaded from IOPscience. Please scroll down to see the full text article.

2007 J. Phys. D: Appl. Phys. 40 1635

(http://iopscience.iop.org/0022-3727/40/6/008)

View the table of contents for this issue, or go to the journal homepage for more

Download details:
IP Address: 140.114.66.106
The article was downloaded on 20/12/2010 at 01:45

Please note that terms and conditions apply.

IOP Publishing Journal of Physics D: Applied Physics
J. Phys. D: Appl. Phys. **40** (2007) 1635–1641 doi:10.1088/0022-3727/40/6/008

The memory characteristics of submicron feature-size PZT capacitors with PtO_x top electrode by using dry-etching

Chun-Kai Huang, Chen-Chan Wang and Tai-Bor Wu

Department of Material Science and Engineering, National Tsing Hua University, Hsinchu, Taiwan, Republic of China

Received 17 November 2006, in final form 14 January 2007
Published 2 March 2007
Online at stacks.iop.org/JPhysD/40/1635

Abstract
Dry etching and its effect on the characteristics of submicron feature-size $PbZr_{1-x}Ti_xO_3$ (PZT) capacitors with PtO_x top electrode were investigated. The photoresist (PR)-masked PtO_x films were etched by an Ar/(20%)Cl_2/O_2 helicon wave plasma. A fence-free pattern with a significantly high etch rate and sidewall slope was obtained by the addition of O_2 into the etching gas mixture, due to the chemical instability of PtO_x and the formation of a PtO_2 passivation layer to suppress redeposition of the etch by-products on the etched surface. The patterned PtO_x electrode can be further used as a hard mask for etching the PZT film, subsequently, with the gas mixture of Ar, CF_4 and O_2. A high etching rate of PZT and a good etching selectivity to PtO_x can be obtained at 30% O_2 addition into the Ar/(50%)CF_4 plasma. The etched capacitors have a steep, 72°, sidewall angle with a clean surface. Moreover, the addition of O_2 into the etching gas can well preserve the properties and the fatigue endurance of PtO_x/PZT capacitors.

(Some figures in this article are in colour only in the electronic version)

1. Introduction

Fabrication of ferroelectric thin film capacitors, such as $PbZr_{1-x}Ti_xO_3$ (PZT) and $Ba_{1-x}Sr_xTiO_3$(BST), is important for application in ferroelectric random access memory (FeRAM) and dynamic random access memory (DRAM), respectively [1, 2].

A noble metal electrode, such as Pt, is usually used in the above capacitors for its good electrical property and high oxidation resistance [3] although other electrodes made with conductive oxide are also considered to resolve the polarization fatigue problem arising from the use of Pt electrodes in PZT capacitors [4]. However, the use of Pt electrodes in high-density memory cells is still not practical because the fine patterning of Pt electrodes by dry etching is very difficult due to the low volatility of the etch products, e.g. $PtCl_x$, and the sidewall redeposition (or fence formation) becomes a troublesome problem in device fabrication [5]. Moreover, the low etch selectivity to photo-resists (PR) also causes a shallow-angle profile of the etched capacitors [6]. Such problems must be solved before Pt films can really be used in high-density memory applications.

To have a sidewall-fence-free etching of Pt, several approaches have been studied, such as etching with resist having a round-head to improve the critical-dimension (CD) gain and taper angle [7] or modifying the PR thickness and slope [8]. Approaches such as employing a hard-mask material such as SiO_2 [9] and Ti-base material [10-12], or utilizing a high–temperature technique with CO_2 gas [13], have also been introduced. Unfortunately, etching of Pt with a hard mask damages the ferroelectric capacitor layers during the formation and removal of the mask. Moreover, for application in high-density FeRAM of submicron feature sizes, the capacitor must be fabricated using a single photo mask for pattern transfer, i.e. one mask per dry etching process, to reduce the cell area [14]. Otherwise, it becomes difficult to obtain high anisotropy during capacitor stack etching without process degradation because the capacitor node-to-node space must also be shrunk down by decreasing the device size [15].

It has been found that PtO_x is a very unstable oxide and can easily be reduced at a moderate temperature in conjunction with the release of highly active oxygen [16, 17]. The chemical instability of PtO_x, however, provides the possibility of using it as a transient template for the fabrication of Pt electrodes

 © 2007 IOP Publishing Ltd Printed in the UK

through the patterning of PtO_x and eliminating the previously mentioned drawbacks in etching Pt electrodes [18]. Therefore, in this study, the dry etching of PtO_x films was investigated and followed by using the patterned PtO_x film as a mask for PZT etching.

2. Experimental procedures

Thin films of PZT (150 nm) and PtO_x (150 nm) were prepared by rf magnetron sputtering on 6 inch Pt/TiN/SiO_2/Si substrates, subsequently. The PZT films were deposited on the electrodized substrate at room temperature and crystallized by rapid thermal annealing (RTA) at 600° in O_2 ambient for 5 min. The PtO_x was then deposited in a gas mixture of $Ar/O_2 = 70/30$. After the thin film deposition, all the test specimens were masked with PR of 1 μm thick for etching study. The helicon wave plasma reactor was utilized. The wafer to be etched was clamped onto an electrostatic chuck (ESC). Helium was flowed into the backside of the wafer to improve the thermal conductivity. The temperature of the stage holder and the chamber was 70 °C and 60 °C, respectively and controlled by recirculation chillers.

Specimens with different top-electrode configuration were used to investigate the etching rates and the etching profiles of the PtO_x and PZT films. In addition to the PR-masked PtO_x films, PR-masked Pt films were also prepared for comparison. The PZT films having 100 nm thick PtO_x top electrode (abbreviate as PtO_x/PZT, hereafter) as the hard mask were then etched in a single step sequence after the etch of PtO_x at the optimized condition for surface profile and electrical properties. The PR-masked PZT were also prepared for etching-rate comparison. The etching stopped at the Pt bottom electrode. After that, the specimens were transferred to the ashing chamber via load-lock and the resist was removed by O_2-plasma etching at 180 °C.

The quantitative data of the etch depth and the critical dimensions of the patterned stacks were measured by a Tencor P-10 long-scan surface profiler. Moreover, the sidewall angle of fully etched features and the etch morphology of the stacks were observed by scanning electron microscopy (SEM). The etching effect on the composition and binding energy state of each element in the thin films was examined by x-ray photoelectron spectroscopy (XPS). The light source was Mg Kα radiation (1253.6 eV), and the spectra were calibrated using C 1 s peak (284.6 eV) from the surface contamination as the internal reference. The ferroelectric properties of the PtO_x/PZT/Pt capacitor stacks, as shown schematically in figure 1, were measured with a TF-Analyzer 2000 FE-Module (aixACCT System). The test devices have a size of $100 \times 100\ \mu m^2$.

3. Results and discussion

3.1. Etching characteristics of PtO_x electrodes

The etching characteristics of the PtO_x and Pt films in the helicon wave system were first investigated. Figure 2 shows the etching rates of the PtO_x and Pt films in a gas mixture $Ar/(20\%)Cl_2$ as a function of source power, bias power and gas pressure, respectively. The total flow rate was fixed at

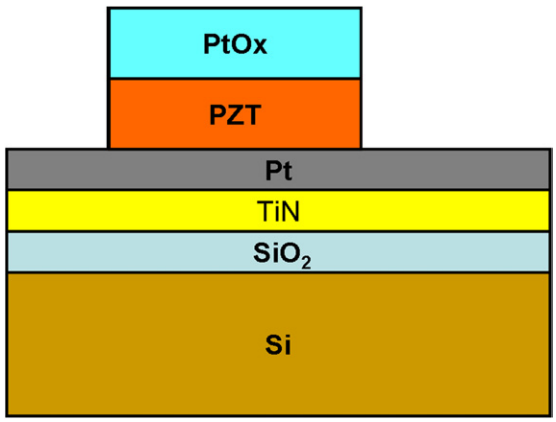

Figure 1. Scheme of PtO_x/PZT/Pt capacitor stack in this study.

40 sccm. The etching rate of PtO_x and Pt films increases by raising the source and bias power, apparently due to the enhancement of chemical activity and bombardment energy of the etch species. The maximum etching rates of the PtO_x and the Pt films were 155 nm min^{-1} and 60 nm min^{-1}, respectively, at a source power of 2100 W and a bias power of 250 W. The etching rate of the PtO_x films is about three times higher than that of the Pt films and increases quite rapidly by raising the source power. A high etching rate of the PtO_x films is also observed for etching under different gas pressures, as shown in figure 2(*c*). However, it increases to a maximum at 5 mTorr and then drops to 120 nm min^{-1} at 10 mTorr. The variation of the etching rates as a function of gas pressure may be attributed to the change of plasma density, i.e. the high-pressure ambient reduces the possibility of gas collisions between the plasma species and leads to a lower plasma density [6].

It has been reported that the employment of O_2 gas in CO/Cl_2 plasma in high-temperature etching can improve the sidewall slope by controlling the deposition of carbon as a protection layer during etching [13]. Therefore, the effect of adding O_2 gas into Ar/Cl_2 plasma on the etching of PtO_x films was investigated. The XPS analysis was employed to explore the mechanism in the suppression of sidewall redeposition in the plasma etching of PtO_x films. Figure 3 shows the XPS spectra of Pt_{4f} electrons from the PtO_x films etched by different gas mixture. From figure 3(*a*), it is clear that the peak of $PtCl_x$ is absent in the spectra of etched PtO_x for the addition of a small amount of O_2 in the Ar/O_2 plasma. The suppression of $PtCl_x$ redeposition can be further verified from the absence of a Cl_{2p} peak in the spectrum of films etched with O_2 added into the plasma, as shown in figure 3(*b*). Moreover, an additional peak corresponding to the PtO_2 phase appears in the Pt_{4f} spectra at a binding energy of 77.3 eV [19], and its intensity increases with increasing O_2 content in the plasma from 5% to 10%, along with a decrease in the intensity of the Pt peak at 71 eV. It indicates that, due to its chemical instability, the PtO_x film can be further oxidized by oxygen plasma to form a PtO_2 layer on the etched surface, which, however, has not been observed in the etching of Pt with oxygen plasma [20]. As the elimination of $PtCl_x$ redeposition is accompanied with the formation of PtO_2, it is believed that the chemical adsorption of $PtCl_x$ molecules must be suppressed due to an *in situ* passivation of the etched surface with the PtO_2 layer formed during etching

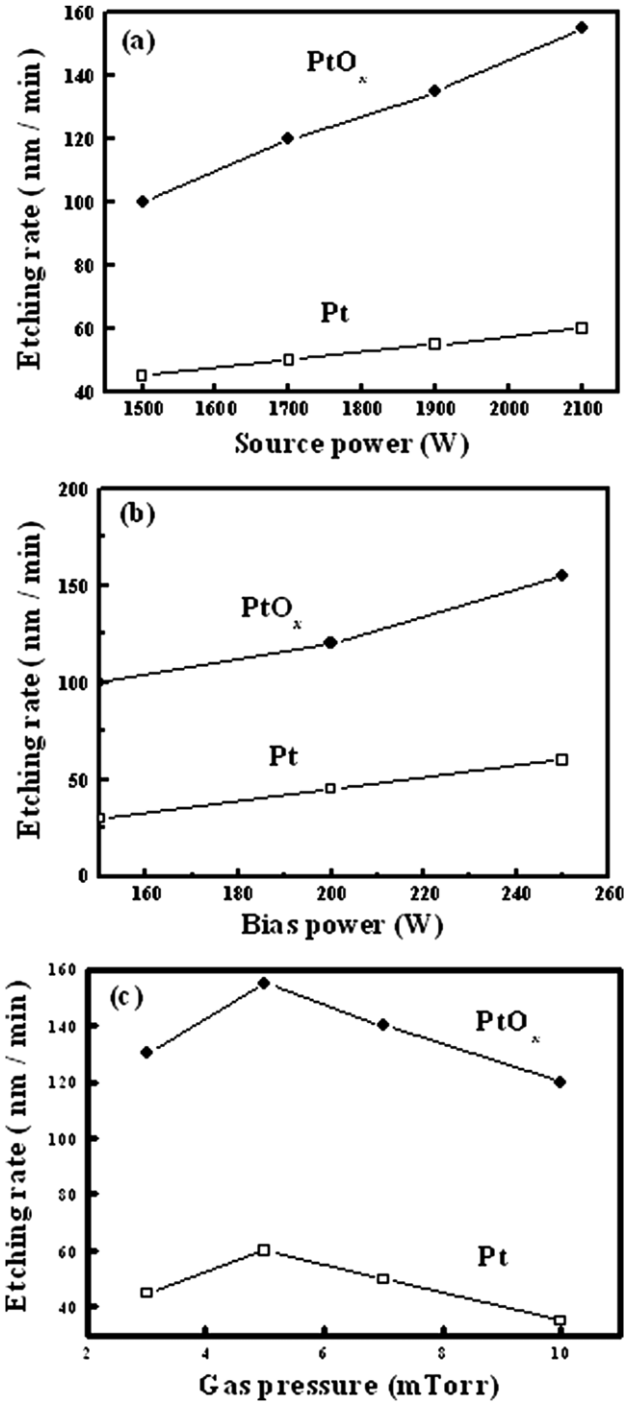

Figure 2. Variation of the etching rate of PtO_x and Pt films as a function of (*a*) source power (with fixed bias power of 250 W, and pressure of 5 mTorr), (*b*) bias power (with fixed source power of 2100 W, and pressure of 5 mTorr) and (*c*) gas pressure (with fixed source power of 2100 W, and bias power 250 W), using a gas flow rate of 40 sccm and a gas mixture of Ar/(20%) Cl_2.

with oxygen-containing plasma. The sidewall redeposition on the etched PtO_x is thus reduced, and a fence-free etching can be obtained with the addition of O_2 into the etching gas mixture, as shown in figure 4. As observed from the SEM micrographs, an etch slope of over 75° was achieved. This result is a significant improvement over previous fence-free etching of PR-marked

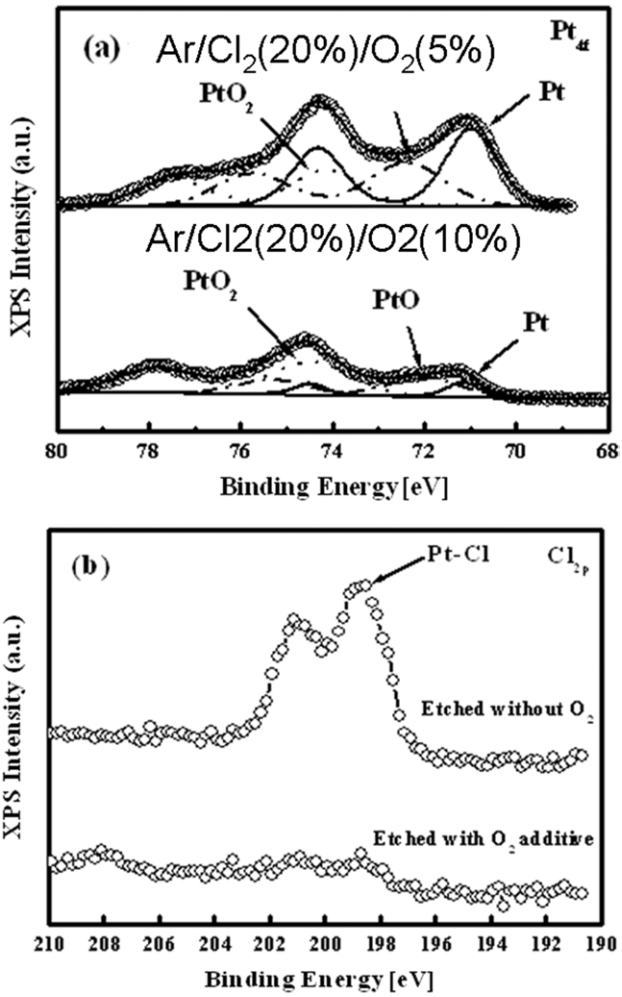

Figure 3. X-ray photoelectron spectra of (*a*) Pt_{4f} electrons from PtO_x films after etching in Ar/Cl_2(20%)/O_2(5%) and Ar/Cl_2(20%) /O_2(10%) plasmas and (*b*) these of Cl_{2p} electrons after etching with or without O_2 addition in the gas mixture.

Pt films with optimized chlorine-base gases having sidewall slopes of less than 45° [21] or, where hard masks other than PR are being used [6].

3.2. Etching characteristics of PtO_x/PZT capacitor stacks

The patterned PtO_x electrode can then be used as a hard mask for etching the PZT films, subsequently. The influence of etching gas on ferroelectric capacitors fabrication is evident as mentioned previously. Therefore, the etching rates and the selectivity of PtO_x/PZT capacitor stacks were studied for etching gas of different compositions. Figure 5 shows the etching rates of PtO_x and PZT and their etching selectivity as a function of Cl_2 content in the Ar/(10%)O_2/Cl_2 plasma. The etching rates of PtO_x and PZT decrease from 180 nm min^{-1} to 150 nm min^{-1} and from 255 nm min^{-1} to 190 nm min^{-1}, respectively, with increasing Cl_2 content up to 60%. The decrease of the etching rate at high chlorine concentration can be attributed to the decrease in Ar ion concentration in the plasma, which reduces the physical bombardment. The selectivity of PZT to PtO_x is also reduced down to 1.26.

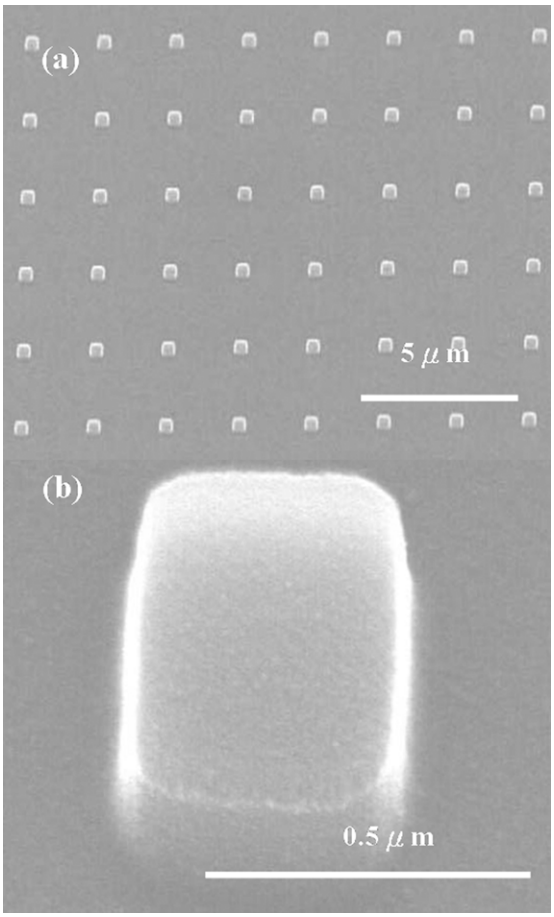

Figure 4. Scanning electron micrograph of (*a*) an array and (*b*) a single PtO_x mesa obtained from etching in Ar/(10%)O_2/(20%)Cl_2 plasma and PR ashing.

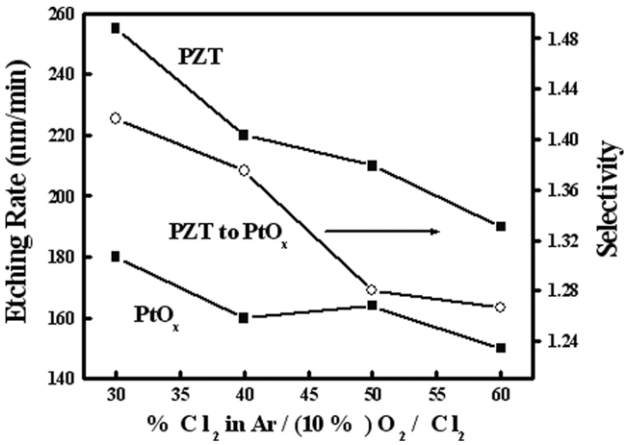

Figure 5. Etch rates of PtO_x and PZT and their selectivity as a function of Cl_2 content in the Ar/(10%)O_2/Cl_2 plasma, using a source power of 2500 W, bias power of 150 W, gas pressure of 5 mTorr and gas flow rate of 40 sccm.

Accordingly, the gas used for PtO_x etching is not suitable for the subsequent etching of PZT films.

Another etching gas with a mixture of Ar, CF_4 and O_2 was then investigated. Figure 6 shows the etch rates of PtO_x and PZT and their etching selectivity as a function of O_2 content in the Ar/(50%)CF_4/O_2 plasma. The maximum etching rate of

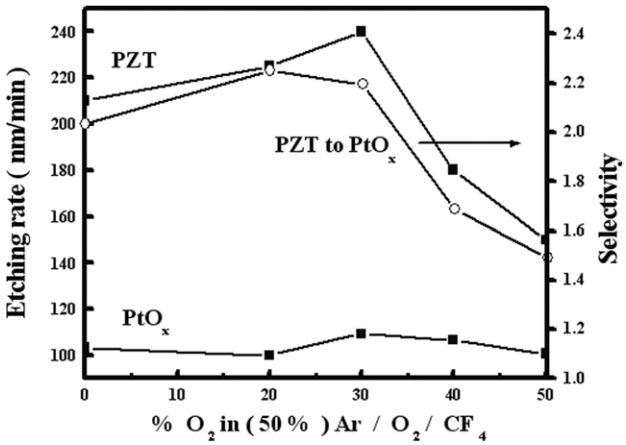

Figure 6. Etch rates of PtO_x and PZT and their selectivity as a function of O_2 content in the Ar/(50%)CF_4/O_2 plasma, using a source power of 2500 W, bias power of 150 W, gas pressure of 5 mTorr and gas flow rate of 40 sccm.

PZT is 240 nm min^{-1} and the etching selectivity to PtO_x can increase to 2.3 at 30% O_2 added into the Ar/(50%)CF_4 plasma. The addition of O_2 into the plasma increases the concentration of fluorine radicals, due to the liberation of fluorine from the reaction of CF_x radicals with O_2 [22]. The corresponding chemical reactions are [23]

$$CF_3 + O \rightarrow COF_2 + F, \quad (1)$$

$$CF_2 + O \rightarrow COF + F. \quad (2)$$

However, the etching rate of the PZT films decreases with increase in the amount of O_2 over 30%. This is consistent with the previous result shown in figure 5 due to the reduction of bombardment from the dilution of Ar plasma.

In contrast, the etching rate of PtO_x in Ar/(50%)CF_4/O_2 gas plasma does not vary significantly, although a maximum etching rate of 105 nm min^{-1} is also found at 30% O_2 addition. This may be because oxygen can be released from PtO_x during etching and reacts with the carbonaceous polymer to form volatile products such as CO and COF_2, [23] giving rise to a less disturbed etching behaviour. Figure 7 shows the SEM micrographs of 0.5 × 0.5 μm^2 PtO_x/PZT capacitor stacks which were plasma-etched with the above two gas mixtures, respectively. Capacitors with steep (72°) sidewall angle and clean surface can be obtained by using the Ar/(50%)CF_4/(30%)O_2 plasma but not for Ar/(10%)O_2/(30%)Cl_2. The result demonstrates that the etching rate and the etching selectivity are important parameters in dry etching of the PtO_x/PZT capacitor stacks, which depend on the choice of etching gas chemistry.

To realize the role of O_2 addition in the etching mechanism for PtO_x/PZT stacks, the etched PZT capacitors with the PtO_x top electrode removed from the specimens were examined by XPS. Figure 8 shows the respective XPS spectra obtained from the PZT capacitors after etching in Ar/(50%) CF_4 and Ar/(30%) O_2/(50%) CF_4 plasma. The Pb_{4f} peak can be deconvoluted into two peaks at 138 eV and 139 eV corresponding to Pb oxide and fluoride, respectively, as shown in figure 8(*a*) [24]. The contribution from Pb-fluoride is clearly eliminated by the addition of O_2 into the Ar/(50%) CF_4

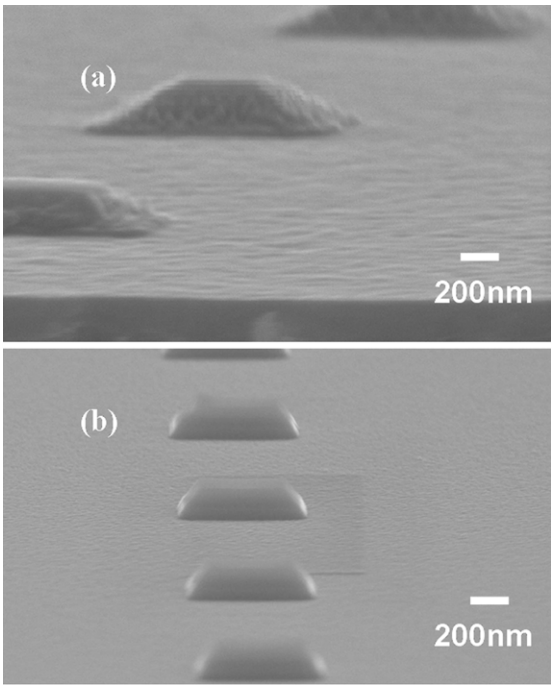

Figure 7. Scanning electron micrographs of PtO_x/PZT capacitor stacks, etched in (*a*) Ar/(10%)O_2/(30%)Cl_2 and in (*b*) Ar/(50%)CF_4/(30%)O_2 plasma. The slope of the capacitor sidewall in (*b*) is 72°.

plasma, indicating that the Pb-fluoride byproducts can be well removed by adding O_2 into the etching gas. The removal of Zr-fluoride by-products by the addition of O_2 can also be observed from the XPS spectra of Zr_{3d} electron shown in figure 8(*b*). The peak intensity of Zr_{3d} increases for etching with O_2-added plasma and the binding energy moves from 183.4 eV towards 181.9 eV, which correspond to Zr-oxyfluoride and Zr-oxide, respectively. Figure 8(*c*) shows the XPS spectrum of Ti_{2d} electron. The contribution from Ti fluoride is not observed in the spectrum, indicating that the byproduct of Ti, i.e. TiF_4, can be well volatilized due to its lower boiling point, i.e. 284° [29]. Figure 9 depicts the change of atomic concentration of Pb, Zr, Ti, O and F, obtained from XPS analysis of the etched PZT capacitors with respect to the content of O_2 in the etching gas. The concentration of F drastically decreases to 3.4% with increasing O_2 content up to 30%, but the concentration of O increases, indicating that the deficiency of oxygen in the etched PZT films can be compensated by adding O_2 into the etching gas.

Figure 10 shows the polarization versus electrical field (P–E) hysteresis loops measured from 100 × 100 μm^2 PtO_x/PZT capacitors etched with or without the addition of O_2 gas in the Ar/(50%) CF_4 plasma. The properties of remanent polarization (P_r) and coercive electrical field (E_c) can be well maintained as the values of unetched capacitors for those etched in plasma with 30%-O_2 addition. However the properties of capacitors etched without O_2 addition significantly degrade along with a clear shift of E_c in the hysteresis loops, which indicates the generation of an internal field (E_i) in the etched films [25]. The magnitude of E_i can be

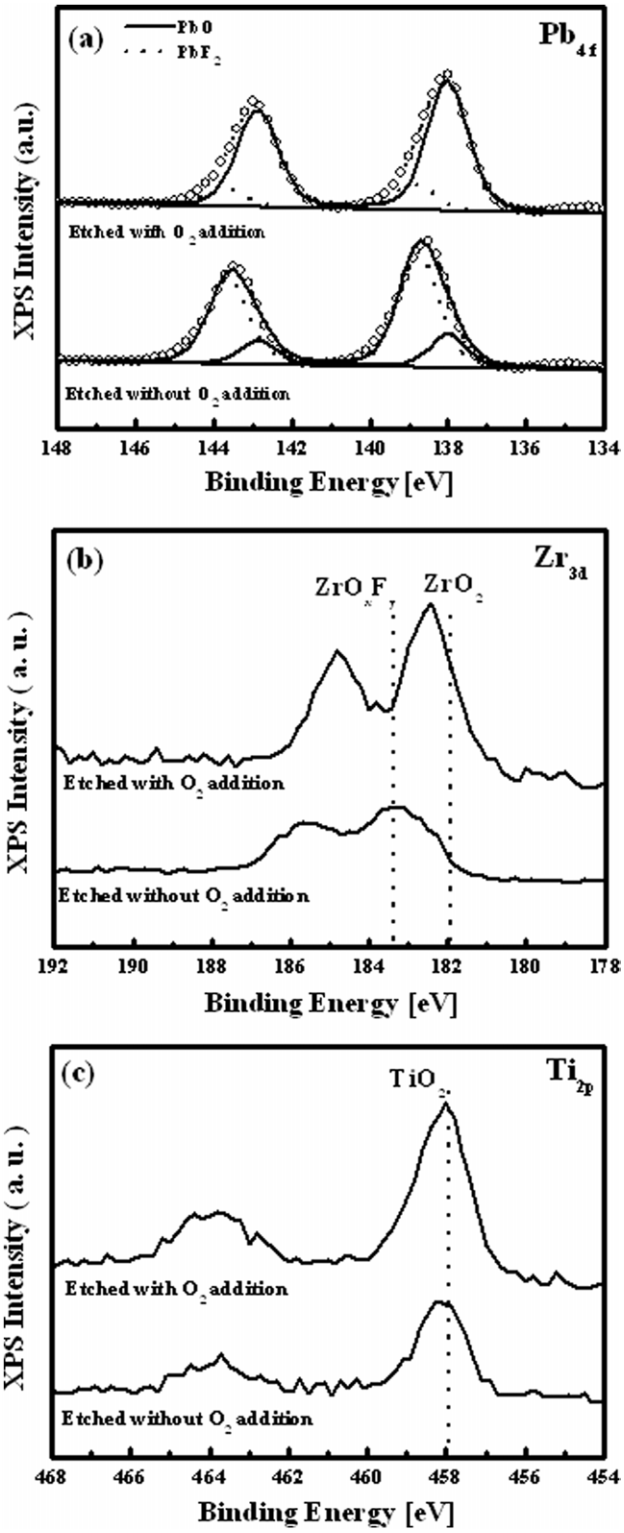

Figure 8. X-ray photoelectron spectra of (*a*) Pb_{4f} electrons, (*b*) Zr_{3d} electrons and (*c*) Ti_{2p} electrons from PZT films after etching in the Ar/CF_4 plasma with or without O_2 addition.

expressed as the following equation:

$$E_i = \frac{|E_{c+}| - |E_{c-}|}{2}, \tag{3}$$

where E_{c+} and E_{c-} are the positive and negative coercive fields, respectively. An E_i value of $-20.55\,kV\,cm^{-1}$ is obtained for

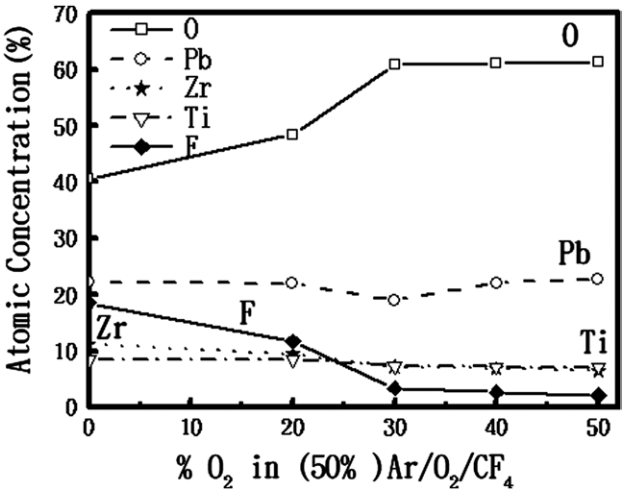

Figure 9. Atomic concentration in the etched PZT capacitors as a function of O_2 concentrations in the Ar/(50%) CF_4 plasma.

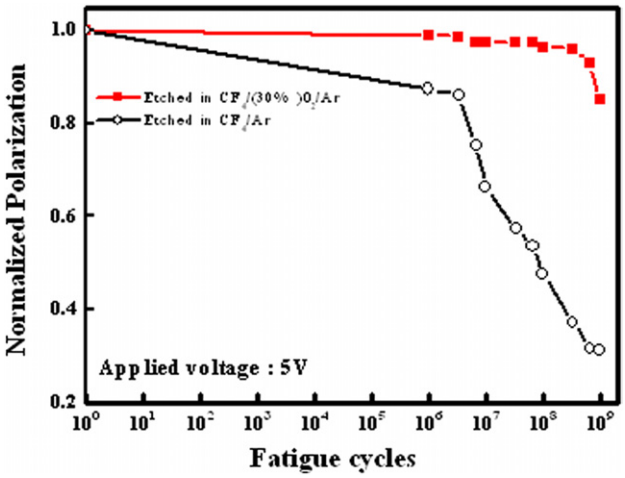

Figure 11. Fatigue characteristics of PtO_x/PZT capacitor stacks ($100 \times 100\ \mu m^2$) etched in Ar/(50%) CF_4 plasma with or without 30% O_2 addition.

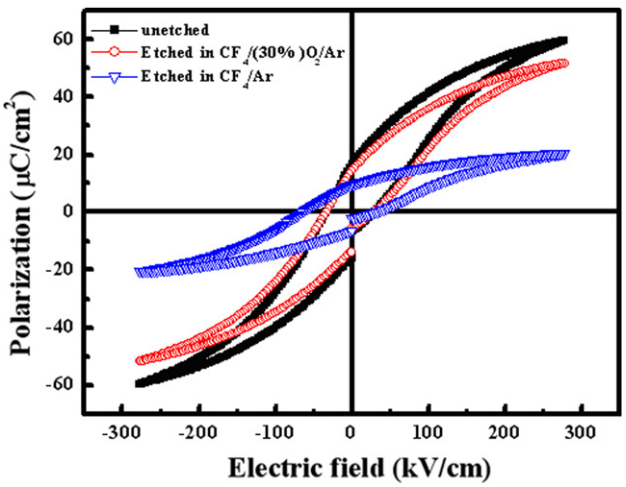

Figure 10. The P–E hysteresis loops of $100 \times 100\ \mu m^2$ PtO_x/PZT capacitors etched with and without the O_2 addition in the Ar/(50%) CF_4 plasma.

the capacitors etched in Ar/(50%) CF_4 plasma, suggesting that the electrical field is built in the direction from the top to the bottom electrode in the etching process. The generation of E_i is attributed to positively charged defects, which are usually the oxygen vacancies, accumulated at the interface between the electrode and the PZT films [26]. For negative E_i, the positive charges must accumulate at the top PtO_x/PZT interface. Because the etch profile of the capacitor stacks is only slightly affected by using the Ar/Cf_4 plasma with or without the addition of 30% O_2 gas (the etching rate and the selectivity are not very different for the two, as shown in figure 6), the drastic loss in polarization is unlikely to be related to the change of dimensions or slopes of the capacitor stacks. It is more likely to be a result of the accumulation of charged defects causing the pinning of the domain wall [27] and the damage of the sidewall by ion bombardment causing the alteration of the local composition [28]. Both of them lead to degradation of the ferroelectric properties. Figure 11 shows the comparisons of fatigue characteristics as a function of the cycle number using a 5 V bipolar square wave with a frequency of 1 MHz. The capacitors etched with oxygen-added plasma show good fatigue endurance up to 10^9 cycles. However, when etched without the addition of O_2, the polarization degrades rapidly, which is apparently related to the increase in oxygen vacancies in the capacitors [27] due to the loss of oxygen in the etching process, as observed from figure 9.

From the above results, it is evident that the removal of the fluoride byproducts is important in improving the etching rate of PZT films. The assistance from physical ion-bombardment in the process is necessary but not sufficient to remove the fluoride byproducts since the fluoride byproducts of PZT elements are low volatile. The chemical contaminations resulting from the fluoride byproducts pile-up on the sidewall would cause parasitic path and reduce the etching rate. On the other hand, the ion bombardment breaks the oxygen bonds in PZT elements causing a loss of oxygen to form oxygen vacancies, which distort the PZT lattice structure and degrade its properties [30]. Therefore, the addition of O_2 in etching gas ambient plays an important role in reducing the byproducts by liberation of fluorine radicals and compensating the oxygen vacancies during the etching process [31].

4. Conclusion

In this study, the etching characteristics of PtO_x electrodes and PtO_x/PZT capacitor stacks were investigated using helicon wave plasma system. A high etch rate, selectivity and etch slope along with a suppression of sidewall redeposition can be obtained in the etching of PR-masked PtO_x film with Ar/(10%)O_2/(20%)Cl_2 plasma. Submicron-feature-size PZT capacitors with steep profiles can also be fabricated by using PtO_x as the top electrode and etched in a Ar/(30%)O_2/(50%)CF_4 gas mixture. For the addition of O_2 in the etching gas, the ferroelectric properties and the fatigue endurance of PtO_x/PZT capacitors can be well preserved. The XPS spectra reveal that the removal of fluoride byproducts is the key to improving the etching rate and preserving the properties of PZT. Therefore, the use of PtO_x as a transient template is an advantage in the

fabrication of submicron-feature-size ferroelectric capacitors with Pt electrodes by dry etching.

Acknowledgments

This work is supported by the Ministry of Economic Affairs of the Republic of China under contract number 92-EC-17-A08-S1-0003. The authors also thank the National Nano Device Laboratory of the National Science Council of the Republic of China for help in carrying out the etching experiment.

Reference

[1] Scott J F, Paz C A de Araujo, McMillan L D, Yoshimori H, Watanabe H, Mihara T, Azuma M, Ueda T, Tetsuk Ueda and Kano G 1992 *Ferroelectrics* **133** 47
[2] Takemura K, Sakuma T and Miyasaka Y 1994 *Appl. Phys. Lett.* **64** 2967
[3] Joshi P C and Krupanidhi S B 1992 *Appl. Phys. Lett.* **61** 1525
[4] Chen M S, Wu T B and Wu J M 1996 *Appl. Phys. Lett.* **68** 1430
[5] Chang L-H, Apen E, Kottke M and Tracy C 1998 *J. Vac. Sci. Technol.* A **16** 1489
[6] Chiang M C, Pan F M, Cheng H C, Liu J S, Chan S H and Wei T C 2000 *J. Vac. Sci. Technol.* A **18** 181
[7] Yunogami T and Kumihashi T 1998 *Jap. J. Appl. Phys.***37**6934
[8] Milkove K R and Wang C X 1997 *J. Vac. Sci. Technol.* A **15** 596
[9] Kwon K-H, Kim C-I, Yun S J and Yeom G-Y 1998 *J. Vac. Sci. Technol.* A **16** 2772
[10] Kim H-w, Ju B-S, Nam B-Y, Yoo W-J, Kang C-J, Ahn T-H, Moon J-T and Lee M-Y 1999 *J. Vac. Sci. Technol.* A **17** 2151
[11] Gutsche M U, Satish D, Athavale W K and Hines D 2000 *J. Vac. Sci. Technol.* B **18** 765
[12] Chung C W and Ilsub C 2000 *J. Vac. Sci. Technol.* A **18** 835
[13] Kim J H, Kim K W and Woo S I 2004 *J. Vac. Sci. Technol.* **B 22** 1662
[14] Shoji K *et al* 1996 *VLSI Tech. Dig.* p 28
[15] Lee S-W *et al* 2002 *Japan J. Appl. Phys.* **41** 6749
[16] Liu T-P, Huang W-P and Wu T-B 2003 *IEEE Trans. Electron Device* **50** 1425
[17] Liu T-P, Huang W-P and Wu T-B 2003 *J. Vac. Sci. Technol.* **A 21** 502
[18] Huang C-K and Wu T-B 2003 *Appl. Phys. Lett.* **83** 3147
[19] Abe Y, Yanagisawa H and Sasaki K 1998 *Japan J. Appl. Phys.* **37** 4482
[20] Kwon K-H, Kang S-Y, Yeom G-Y, Hong N-K and Lee J H 2000 *J. Electrochem. Soc.* **147** 1807
[21] Yoo W J, Hahm J H, Kim H W, Jung C O, Koh Y B and Lee M Y 1996 *Japan J. Appl. Phys.* **35** 2501
[22] Kim J-W, Kim Y-C and Lee W-J 1995 *J. Appl. Phys.* **78** 2045
[23] Grill A 1994 *Cold plasma in materials fabrication* (IEEE Press, New York, 1994).
[24] Jung J-K and Lee W-J 2001 *Japan J. Appl. Phys.* **40** 1408
[25] Chung C W and Kim C J 1997 *Japan. J. Appl. Phys.* **36** 2747
[26] Lee E G, Wouters D J, Willems G and Maes H E 1996 *Appl. Phys. Lett.* **69** 1223
[27] Soyer C, Cattan E, Rèmiens D and Guilloux-Viry M 2002 *J. Appl. Phys.* **92** 1048
[28] Lee J K, Kim T-Y, Chung I and Desu S B 1999 *Appl. Phys. Lett.* **75** 334
[29] Lin Y-y, Liu Q, Tang T-a and Yao X 2000 *Appl. Surf. Sci.* **165** 34
[30] Kang M-G, Kim K-T and Kim C-I 2001 *Thin Solid Films* **398–399** 448
[31] Jang H K, Lee S K, Cheol Eui Lee, Noh S J and Lee W I 2000 *Appl. Phys. Lett.* **76** 882